

Learning from History: Task-agnostic Model Contrastive Learning for Image Restoration

Gang Wu, Junjun Jiang *, Kui Jiang, Xianming Liu

School of Computer Science and Technology, Harbin Institute of Technology, Harbin 150001, China
 {gwu, jiangjunjun, jiangkui, csxm}@hit.edu.cn

Abstract

Contrastive learning has emerged as a prevailing paradigm for high-level vision tasks, which, by introducing properly negative samples, has also been exploited for low-level vision tasks to achieve a compact optimization space to account for their ill-posed nature. However, existing methods rely on manually predefined, task-oriented negatives, which often exhibit pronounced task-specific biases. In this paper, we propose an innovative approach for the adaptive generation of negative samples directly from the target model itself, called “learning from history”. We introduce the Self-Prior guided Negative loss for image restoration (SPNIR) to enable this approach. Our approach is task-agnostic and generic, making it compatible with any existing image restoration method or task. We demonstrate the effectiveness of our approach by retraining existing models with SPNIR. The results show significant improvements in image restoration across various tasks and architectures. For example, models retrained with SPNIR outperform the original FFANet and DehazeFormer by 3.41 dB and 0.57 dB on the RESIDE indoor dataset for image dehazing. Similarly, they achieve notable improvements of 0.47 dB on SPA-Data over IDT for image deraining and 0.12 dB on Manga109 for a $4\times$ scale super-resolution over lightweight SwinIR, respectively. Code and retrained models are available at <https://github.com/Aitical/Task-agnostic-Model-Contrastive-Learning-Image-Restoration>.

Introduction

Image restoration, aiming at recovering a high-quality image from the degraded one, is a fundamental problem in the fields of image processing and computer vision (Yang et al. 2021; Wang, Chen, and Hoi 2021a; Jiang et al. 2023). Deep learning approaches have brought about considerable advancements in image restoration while there are still challenges due to its ill-posed nature (Wang, Chen, and Hoi 2021b; Lu et al. 2023). The success of self-supervised learning paradigm for high-level tasks, especially those contrastive learning methods, has drawn great attention (Gui et al. 2023a). This inspires many researchers to make strides in improving the end-to-end learning paradigm for image restoration tasks, incorporating the concept of sample contrastive learning and bridging the gap between high-level and low-level tasks (Wu et al. 2021; Chen et al. 2022b; Ye

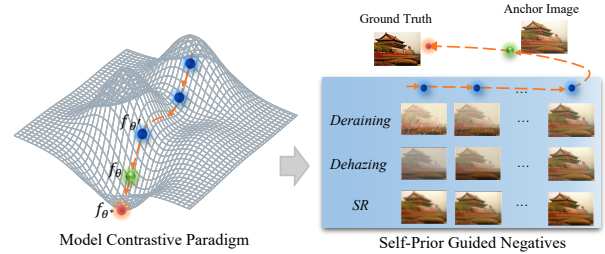


Figure 1: Illustration of the proposed model contrastive paradigm. We provide a common optimization space for it. To the target model f_θ , the proposed model contrastive paradigm exploits negative samples from the latency model $f_{\theta'}$ smoothly. Compared to task-oriented negatives in previous work, our model contrastive paradigm is task-agnostic and general to various image restoration tasks. This provides a compact optimization space adaptively (pushing target model f_θ closer to assumed optimal f_{θ^*}).

et al. 2022; Wu, Jiang, and Liu 2023; Zheng et al. 2023). Image restoration tasks usually contain high-quality ground truth as learning target (positive sample), and more attention is paid on mining appropriate negative examples. For instance, Wu *et al.* (Wu et al. 2021) directly utilized the low-quality input as the negative sample and introduced the contrastive paradigm for the image dehazing task. Wu *et al.* proposed a hard negative construction for image super-resolution tasks. Compared to the super-resolved results, hard negatives with similar image quality to the anchor sample can push it ahead effectively (Wu, Jiang, and Liu 2023). Most recently, Zheng *et al.* proposed a progressively improved negative lower bound for image dehazing, employing multiple pre-trained models to provide consensual negatives (Zheng et al. 2023).

While existing contrastive learning paradigms, leveraging potent approaches like hard negative mining (Wu, Jiang, and Liu 2023) and curriculum learning strategies (Zheng et al. 2023), have shown impressive performance, certain intrinsic limitations persist. Chiefly, there exists an *over-reliance on task-oriented prior*, leading to limited generalization capability across multiple image restoration tasks. Many existing methods exhibit a pronounced task-oriented bias, where negative sample generation is often influenced by prior knowledge and empirical evaluation centered around a singular

*Corresponding Author

target task (Wu, Jiang, and Liu 2023; Zheng et al. 2023). Such approaches, while effective in isolation, often impede to a diverse set of image restoration tasks and model architectures. In light of these challenges, it compels us to ask: *Is there a task-agnostic, general method for negative sampling that could potentially enhance the performance of a diverse range of image restoration tasks?*

Taking this into consideration, let us turn our attention from sample selection into the target model itself. In recent literature, much of the spotlight has been directed towards sample selection, often overlooking a latent gem—the latency model—during the learning process. Specifically, the latency model, when operating within a close optimization step, shares strikingly similar parameters with the current model. This intrinsic similarity paves the way for the construction of adaptive negatives pertinent to the current anchor sample. To illustrate this concept, we introduce a toy example in Fig. 1. It becomes evident that, throughout the learning journey, the output of the latency model exhibits a sub-optimal but congruent distribution relative to the current anchor sample. This alignment offers the potential to derive ‘hard’ negatives that are well-suited to the task at hand. Furthermore, as the entire learning process is incrementally refined, the negatives in our model contrastive paradigm adopt a curriculum way naturally. Motivated by these insights, we put forth an innovative *model contrastive paradigm* for image restoration tasks. In contrast to the previous approaches with complex negative mining strategies, the core of our proposed model contrastive paradigm lies in the self-promoted negatives between latency and current models. Notably, it is task-agnostic, adaptive, and general to existing methods and various image restoration tasks.

In detail, we proposed a model contrastive paradigm for various image restoration tasks by a **Self-Prior** guided Negative loss (simplified as SPN). Importantly, the proposed SPN is compatible with existing approaches across different architectures and target tasks. We apply and retrain existing models by the proposed model contrastive. As presented in Fig. 2, one can find that the proposed SPN achieves promising improvements across multiple tasks and architectures. More specifically, based on the lightweight EDSR (Lim et al. 2017) and SwiniR (Liang et al. 2021), our retrained models display superior performance on Manga109 test dataset for $\times 4$ scale image super resolution, boasting improvements of **0.16 dB** and **0.12 dB** in term of PSNR. Retrained IDT (Xiao et al. 2022) achieves **0.38 dB** and **0.7 dB** gains on Rain200L and SPA datasets for image deraining. Moreover, for image dehazing, we gain a notable improvement of **3.41 dB** and **0.57 dB** compared to the original FFANet (Qin et al. 2020a) and DehazeFormer (Song et al. 2023), respectively.

The main contributions of this work are:

- The paper proposes a novel approach to negative sample construction for image restoration tasks through a task-agnostic model contrastive paradigm. Unlike conventional methods that manually apply negative samples to specific target task, the proposed model contrastive paradigm exhibits versatility across multiple tasks and models.

- The paper introduces the Self-Prior guided Negative loss for Image Restoration (SPNIR), which departs from existing methods that rely on manually predefined, task-oriented negatives. The SPNIR pioneers an innovative approach for the adaptive generation of negative samples directly from the target model itself.
- The paper demonstrates the effectiveness of the proposed approach by retraining existing models with the SPNIR, which significantly improves image restoration across various tasks and architectures.

Related Work

Image Restoration Image restoration, aiming at recovering a high-quality image from the degraded one, is a fundamental problem in the fields of image processing and computer vision. It is indispensable in several domains, including photography, surveillance, medical imaging, and remote sensing (Su, Xu, and Yin 2022). In recent years, approaches based on deep learning have emerged as potent tools, providing significant advances for image restoration (Wang, Chen, and Hoi 2021a; Jiang et al. 2023; Wang et al. 2021a; Gui et al. 2023b). Among these, Convolutional Neural Networks (CNN) have been utilized, resulting in a plethora of methods designed to address various image restoration tasks (Dong et al. 2016; Zhang et al. 2017; Zhang, Zuo, and Zhang 2018; Yang et al. 2017a). Furthermore, remarkable strides have been made by the development of a spectrum of deep models, including proposals for residual or dense architectures (Lim et al. 2017; Zhang et al. 2018b), the integration of attention mechanisms (Zhang et al. 2018a; Liu et al. 2019; Dai et al. 2019), and the implementation of UNet-based architectures (Ronneberger, Fischer, and Brox 2015; Jiang et al. 2020). In addition, some work explored the attention mechanism to boost the performance for image super-resolution (Zhang et al. 2018a; Liu et al. 2018; Mei, Fan, and Zhou 2021), image deraining (Li et al. 2018a; Wang et al. 2019a), image deblurring (Suin, Purohit, and Rajagopalan 2020), and so on. On the frontier of recent development, Transformer architectures achieves significant breakthroughs in computer vision (Liu et al. 2021; Dosovitskiy et al. 2021). This trend has spurred the development of Transformer-based interventions for image restoration tasks such as image super-resolution (Liang et al. 2021), image dehazing (Song et al. 2023; Zamir et al. 2022), image deraining (Xiao et al. 2022), image deblurring (Wang et al. 2022), and low-light image enhancement (Wang et al. 2023). We are witnessing a surge in the performance of increasingly complex architectures and there is a growing demand for applications in real-world systems. Many researcher have turned attention to lightweight methods (Jiang et al. 2021; Lamba and Mitra 2021; Hui et al. 2019; Wu et al. 2023b; Lu et al. 2022; Wu et al. 2023a).

Contrastive Learning Self-supervised learning has achieved great success in high-level vision tasks, especially those contrastive learning methods (Gui et al. 2023a; He et al. 2020; Chen et al. 2020; Grill et al. 2020; Chen and He 2021). For low-level image restoration tasks, many

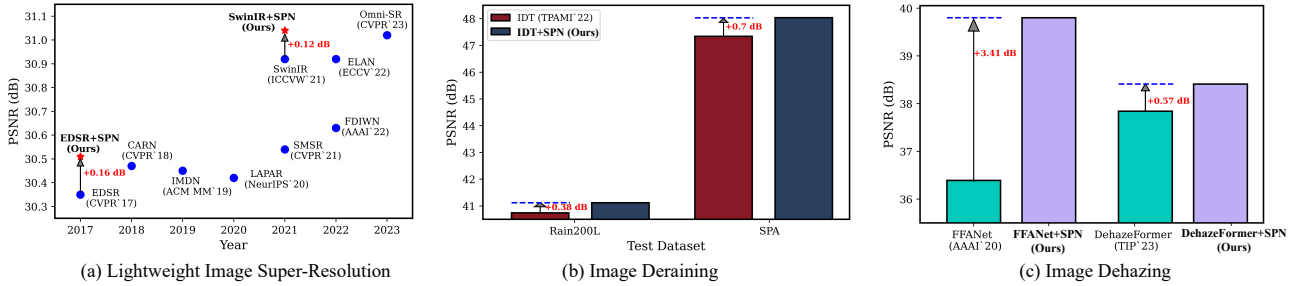


Figure 2: Comparisons between models retrained by our proposed model contrastive paradigm and the originals. Retrained models can achieve remarkable improvements on various image restoration tasks. Details are provided in Section Experiment

researchers attempted to bridge the gap between low-level and high-level tasks and exploit more self-supervised information to promote image restoration tasks (Wang et al. 2021b; Wu et al. 2021; Chen et al. 2022b; Ye et al. 2022; Zheng et al. 2023; Wu, Jiang, and Liu 2023). Wang *et al.* introduced the contrastive learning method into the blind image super-resolution, which proposes an unsupervised degradation estimation encoder by contrastive pretraining (Wang et al. 2021b). In contrast to unsupervised learning for high-level vision tasks, low-level tasks usually have high-quality ground-truth images. Discovering and Leveraging negative samples is crucial for low-level contrastive paradigm. Wu *et al.* took the input low-quality as the negative sample and proposed a perceptual-based contrastive loss to achieve a more compact convergence space (Wu et al. 2021). For unsupervised image deraining, Chen *et al.* leveraged contrastive loss by discriminating different generated degradation (Chen et al. 2022b), and Ye *et al.* incorporated self-similarity within the image and proposed a local patch contrastive loss (Ye et al. 2022). Wu *et al.* proposed a practical contrastive learning framework for super-resolution single image and proposed the hard negative construction (Wu, Jiang, and Liu 2023). By interpolating the negative information, they further improve the performance for target task. However, adaptation and generalization of these methods to different image restoration models and tasks are limited.

In this work, we introduce an innovative model contrastive paradigm for image restoration by a self-prior guided negative loss. The proposed approach is task-agnostic and compatible with existing methods and provides significant improvements over various image restoration tasks.

Method

Overall Framework

Deep learning-based image restoration methodologies have recently made considerable breakthroughs across multiple restoration tasks, including image super-resolution, image dehazing, image deblurring, image deraining, and so on. In this paper, we focus our attention on the vanilla end-to-end learning process in deep learning methods. To facilitate clarity, we provide a succinct illustration of the end-to-end image restoration framework, visualized in Fig. 3 (a). Given a low-quality input image denoted as I^{LQ} , the target model f_θ processes this input to produce a reconstructed image,

I^{Rec} . Concurrently, its high-quality counterpart is denoted by I^{HQ} . The training of the target model is steered by the minimization of the loss \mathcal{L}_{rec} . Delving further, Fig. 3 (b) showcases various contrastive learning strategies tailored for image restoration tasks. These approaches harness the power of negative samples, augmented by the negative regularization \mathcal{L}_{neg} (Wu et al. 2021; Zheng et al. 2023; Wu, Jiang, and Liu 2023).

In this paper, we propose an innovative model contrastive paradigm for image restoration tasks, shown in Fig. 3 (c). Instead of utilizing predefined negative samples, we craft our negatives directly from the target model. At this point, we denote the target model f_θ , indicative of the optimized one at the current training iteration t . Subsequently, we employ a distinct step, s , to establish a latency model $f_{\theta'}$, also referred to as the negative model, to generate adaptive negative samples for the training of the target model. The overall pipeline is straightforward, and the detailed implementation of negative models and associated loss functions will be discussed in the subsequent sections.

Learning from History

The most direct approach entails saving multiple model checkpoints and subsequently reloading them to function as the latency negative model. However, this approach presents two significant challenges: Firstly, a substantial gap might exist between the saved checkpoints and the target model. This discrepancy could potentially undermine the effectiveness of the negative regularization. Secondly, it is unfeasible to process the latency model too frequently, particularly in the context of recent, large models.

In light of these obstacles, we introduce an efficient technique to achieve a smooth negative model, leveraging the strategy of exponential moving averages (EMA). The update equation for the negative model is:

$$\begin{aligned} \theta' &= w\theta' + (1-w)\theta, \\ \text{s.t. } t\%s &= 0. \end{aligned} \quad (1)$$

In this schema, w denotes the update weight, s is the update step, and t captures the current iteration. To ensure the preservation of latency parameters, we adopt a long step s and selectively update the negative model f_θ at intervals of every s iterations.

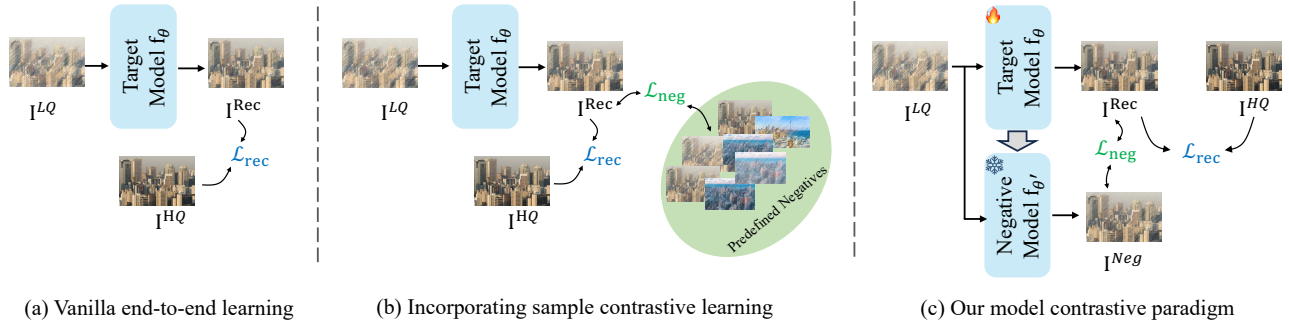


Figure 3: Comparisons of different learning paradigms for image restoration tasks. (a) Depicts the vanilla end-to-end learning paradigm, where target image restoration models are trained with supervised reconstruction loss; (b) Illustrates the sample contrastive paradigm adopted in existing methods, leveraging additional information from manually defined negative samples; (c) Showcases our model contrastive paradigm, which generates negative samples from the latency target model, providing a task-agnostic and adaptive approach to various image restoration tasks.

Self-Prior Guided Negative Loss

At the heart of our model contrastive paradigm, a loss function mediates between the target reconstruction I^{Rec} and its negative counterpart, I^{Neg} . Herein, we take the pre-trained VGG (Simonyan and Zisserman 2015) network as the embedding network to map the samples into a latent feature space, where $f^{Rec} = \text{VGG}(I^{Rec})$ and $f^{Neg} = \text{VGG}(I^{Neg})$. Then the proposed negative loss \mathcal{L}_{neg} is formulated as

$$\mathcal{L}_{neg} = \|f^{Rec} - f^{Neg}\|_1. \quad (2)$$

Furthermore, our model-based contrastive paradigm can incorporate multiple negatives by adding more negative models. For more robustness, we take multiple distinct steps to obtain several latency models. The combined negative loss, accounting for multiple negatives, is represented as

$$\mathcal{L}_{neg}^N = \frac{1}{N} \sum_{i=1}^N \|f^{Rec} - f_i^{Neg}\|_1, \quad (3)$$

where N denotes the total number of negative models and f_i^{Neg} corresponds to the latent feature of the i th negative sample.

Compared to existing methods, our negative regularization is a self-prior guided loss function, where the negative samples stem from the target model itself. More important, it is general and transferable to existing image restoration models while retaining the original learning strategy. Typically, image restoration tasks utilize a reconstruction loss, \mathcal{L}_{rec} , relying on metrics such as Mean Absolute Error (MAE) and Mean Squared Error (MSE). To validate the prowess of our model-based contrastive paradigm by \mathcal{L}_{neg} , we have retrained numerous exiting methods with it, testing across different image restoration tasks and architectures. The precise formulation of the reconstruction loss \mathcal{L}_{rec} is contingent on the method under retraining.

Generally, the total loss function within our model-based contrastive paradigm is defined as:

$$\mathcal{L} = \mathcal{L}_{rec} - \lambda \mathcal{L}_{neg}^N, \quad (4)$$

where \mathcal{L}_{rec} represents the corresponding reconstruction loss adopted in existing method, and λ is the balancing coefficient. This simple formulation allows us to incorporate the proposed SPN with existing image restoration methods, enhancing their flexibility and adaptability to various tasks.

Remark

In this study, we introduce an innovative model contrastive paradigm that focus on the target model itself. This approach significantly simplifies the construction of negatives while simultaneously providing adaptive and effective ones. Contrary to existing approaches (Wu et al. 2021; Wu, Jiang, and Liu 2023; Zheng et al. 2023), the proposed model contrastive paradigm does not rely on the restrictions of task-oriented priors, making it versatile and universal to various image restoration tasks. In essence, our contribution lies in providing a task-agonist and general approach to the construction of negative samples, expanding the scope of contrastive learning in the field of image restoration.

Experiment

Experimental Settings

Image Super-Resolution We retrain the CNN-based EDSR (Lim et al. 2017) and Transformer-based SwinIR (Liang et al. 2021). We take 800 images from DIV2K (Agustsson and Timofte 2017) for training and test them on five benchmark datasets.

Image Dehazing We employ the CNN-based FFANet (Qin et al. 2020a) and Transformer-based DehazeFormer (Song et al. 2023) as our baselines and retrain them for image dehazing tasks. Following (Song et al. 2023), we utilize the indoor training dataset (ITS) and RESIDE-6K to separately train the models and evaluate on the synthetic objective testing set (SOTS).

Image Deblurring For image deblurring, we retrain and evaluate NAFNet (Chen et al. 2022a) on GoPro dataset.

Image Deraining For image deraining, we conduct experiments on several publicly available benchmarks, namely Rain200L/H (Yang et al. 2017b), DID-Data (Li et al. 2018b), DDN-Data (Fu et al. 2017), and SPA-Data (Wang et al. 2019b). We adopt the Transformer-based IDT model (Xiao

Method	Architecture	Scale	Avg.	Set14	B100	Urban100	Manga109
			PSNR/SSIM	PSNR/SSIM	PSNR/SSIM	PSNR/SSIM	PSNR/SSIM
EDSR-light	CNN	×2	32.06/0.9303	33.57/0.9175	32.16/0.8994	31.98/0.9272	30.54/0.9769
+SPN (Ours)			32.19/0.9313	33.67/0.9182	32.21/0.9001	32.23/0.9297	30.64/0.9772
EDSR-light		×4	28.14/0.8021	28.58/0.7813	27.57/0.7357	26.04/0.7849	30.35/0.9067
+SPN (Ours)			28.21/0.8040	28.63/0.7829	27.59/0.7369	26.12/0.7878	30.51/0.9085
SwinIR-light	Transformer	×4	28.46/0.8099	28.77/0.7858	27.69/0.7406	26.47/0.7980	30.92/0.9151
+SPN (Ours)			28.55/0.8114	28.85/0.7874	27.72/0.7414	26.57/0.8010	31.04/0.9158
SwinIR		×4	28.88/0.8190	28.94/0.7914	27.83/0.7459	27.07/0.8164	31.67/0.9226
+SPN (Ours)			28.93/0.8198	29.01/0.7923	27.85/0.7465	27.14/0.8176	31.75/0.9229

Table 1: **Comparison results of image super-resolution.** We take CNN-based EDSR (Lim et al. 2017) and Transformer-based SwinIR (Liang et al. 2021) as our baselines. Results of retrained models by the proposed model contrastive paradigm are in **bold**. Avg. presents the mean value of four test datasets.

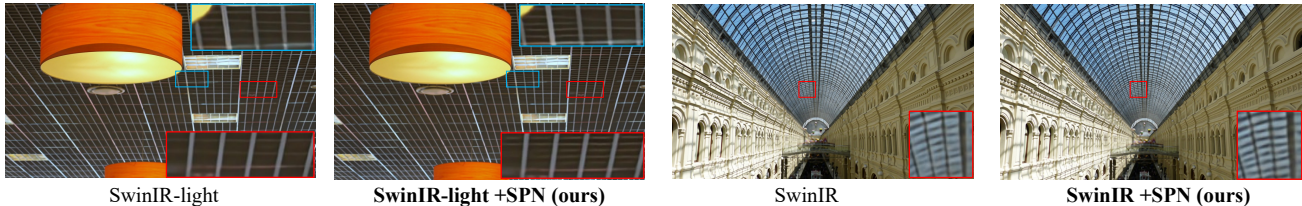


Figure 4: Visual comparison for image super-resolution tasks. Displayed are results from both the original SwinIR models and those retrained by our model contrastive paradigm. The enhancements brought about by our approach are clearly evident.

et al. 2022) as our baseline and subsequently retrain it using the proposed model contrastive paradigm.

Given the diverse training settings across various image restoration tasks, we ensure a fair comparison by strictly adhering to the original training configurations of each retrained model, as specified in their literature.

Comparison Results

Image Super-Resolution We first investigate the image super-resolution task, utilizing both CNN-based EDSR and Transformer-based SwinIR as baselines to evaluate our proposed Self-Prior guided Negative regularization (SPN). Results presented in Tab. 1 across various architectures and model capacities. Our proposed model contrastive paradigm can achieve considerable improvements when retraining lightweight models such as EDSR and SwinIR, achieving average gains of 0.07 dB and 0.09 dB on scale ×4, respectively. Moreover, the retrained EDSR model demonstrates a noteworthy average improvement of 1.3 dB for the scale ×2 task. Notably, there are substantial improvements by our retrained on the Urban100 and Manga109 datasets. This implies that our model contrastive paradigm facilitates a more accurate and compact convergence in the restoration process. Moreover, comparisons with current state-of-the-art methods are presented in Fig. 2 (a). Remarkably, the retrained EDSR and SwinIR can eclipse the performance of several contemporary methods. These underscore the promise of our model contrastive paradigm.

In addition to the lightweight models, we also retrain the large SwinIR model. Our proposed approach exhibits its general applicability to larger models, providing an average improvement of 0.05 dB. It is worth noting that the improvements seen in larger models were relatively smaller when compared to the lightweight models. This observation is consistent with the understanding that lightweight mod-

els, owing to their smaller capacity, may struggle to find an optimal solution. Therefore, our proposed model contrastive paradigm provides significant assistance in these cases. Conversely, larger models have the capacity to fit or even overfit the dataset, hence the model contrastive paradigm improves them within a lesser margin. Visual results are showcased in Fig. 4. It is also evident that our model contrastive paradigm can improve existing methods, particularly in bringing more precise textures.

Image Deraining We take the state-of-the-art IDT (Xiao et al. 2022) as the baseline and retrain it by the proposed model contrastive paradigm on five datasets, and Tab. 2 provides a comprehensive comparison. The retrained IDT, achieves an average PSNR improvement of 0.26 dB across all test datasets. For instance, it showcase a gain of 0.7 dB in comparison to its original on SPA dataset. Furthermore, visual results are illustrated in Figure 5, accompanied by a divergence map. It intuitively highlights the enhancements in the degraded regions. These insights underscore the capability of our model contrastive paradigm to refine the target degradation.

Image Dehazing Following the recent work (Song et al. 2023), we utilize the SOTS-indoor and SOTS-mix datasets for testing. In detail, we retrain FFANet (Qin et al. 2020b) and DehazeFormer (Song et al. 2023), with the outcomes detailed in Fig. 3. From the table, a remarkable enhancement is achieved over FFANet, exhibiting gains of 3.41 dB and 0.69 dB on the indoor and mixed test datasets, respectively. Concurrently, the Transformer-based model IDT also record advancements, evident across various model scales. Specifically, the retrained DehazeFormer-B achieves the most pronounced improvement of 0.57 dB on the indoor test dataset. Intriguingly, the retrained FFANet even outperforms the DehazeFormer. It is reasonable that FFANet is a CNN-based model, which has a large model capacity with heavy param-

Method	Avg. PSNR/SSIM	Rain100L PSNR/SSIM	Rain100H PSNR/SSIM	DID PSNR/SSIM	DDN PSNR/SSIM	SPA PSNR/SSIM
(CVPR'21) MPRNet	36.17/0.9543	39.47/0.9825	30.67/0.9110	33.99/0.9590	33.10/0.9347	43.64/0.9844
(AAAI'21) DualGCN	36.69/0.9604	40.73/0.9886	31.15/0.9125	34.37/0.9620	33.01/0.9489	44.18/0.9902
(ICCV'21) SPDNet	36.54/0.9594	40.50/0.9875	31.28/0.9207	34.57/0.9560	33.15/0.9457	43.20/0.9871
(CVPR'22) Uformer-S	36.95/0.9505	40.20/0.9860	30.80/0.9105	34.46/0.9333	33.14/0.9312	46.13/0.9913
(CVPR'22) Restormer	37.49/0.9530	40.58/0.9872	31.39/0.9164	35.20/0.9363	34.04/0.9340	46.25/0.9911
(CVPR'23) DRSformer	38.33/0.9676	32.17/0.9326	41.23/0.9894	35.35/0.9646	34.35/0.9588	48.54/0.9924
(TPAMI'23) IDT	37.77/0.9593	40.74/0.9884	32.10/0.9343	34.85/0.9401	33.80/0.9407	47.34/0.9929
(Ours) IDT+SPN	38.03/0.9610	41.12/0.9893	32.17/0.9352	34.94/0.9424	33.90/0.9442	48.04/0.9938

Table 2: **Comparison results of image deraining.** We take IDT (Xiao et al. 2022) as the benchmark and retrain it with the proposed model contrastive paradigm. We evaluate the performance on several image deraining datasets, and our results are in **bold** (Average performance of the five datasets is calculated in the Avg. column).



Figure 5: Visual comparisons between IDT and our retrained one. A divergence map delineates the differences, highlighting the improvement achieved by ours, particularly in degraded regions.

Methods	ITS		RESIDE-6K	
	SOTS-indoor		SOTS-mix	
	PSNR	SSIM	PSNR	SSIM
(CVPR'21) AECR-Net	37.17	0.990	-	-
(ICLR'23) SFNet	41.24	0.996	-	-
(CVPR'23) C ² PNet	42.56	0.995	-	-
(AAAI'20) FFANet	36.39	0.989	29.96	0.973
(Ours) FFANet+SPN	39.80	0.995	30.65	0.976
(TIP'23) DehazeFormer-T	35.15	0.989	30.36	0.973
(Ours) DehazeFormer-T+SPN	35.51	0.990	30.44	0.974
(TIP'23) DehazeFormer-S	36.82	0.992	30.62	0.976
(Ours) DehazeFormer-S+SPN	37.24	0.993	30.77	0.978
(TIP'23) DehazeFormer-B	37.84	0.994	31.45	0.980
(Ours) DehazeFormer-B+SPN	38.41	0.994	31.57	0.981

Table 3: **Comparison results of image dehazing.** Results of our retrained models are in **bold**.

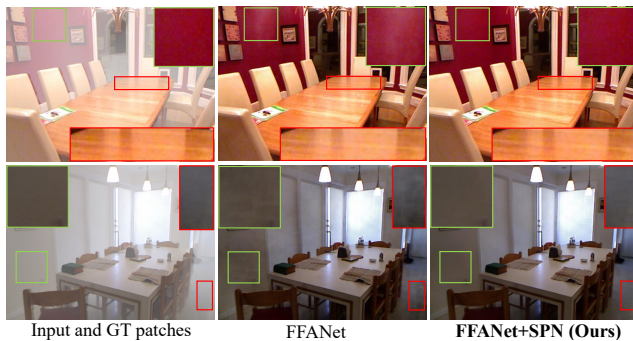


Figure 6: Visual results of FFANet and our retrained one for image dehazing.

eter counts, and our model contrastive paradigm appears to steer FFANet towards more optimized results. Some visual

results are presented in Fig. 6. One can find that retrained FFANet is clearer with less artifacts.

Image Deblurring Results of the retrained NAFNet (Chen et al. 2022a) for image deblurring are in Tab. 4. One can find that the retrained NAFNet showcases notable enhancements compared to the original and outperforms the Transformer-based Restormer (Zamir et al. 2022).

Comparison to Existing Sample Contrastive Paradigm

In contrast to existing methods that employ task-oriented negatives, our model contrastive paradigm provides straightforward enhancement to image restoration tasks. We furnish a comprehensive comparison between existing contrastive approaches and our innovative model contrastive paradigm. For image dehazing task, we examine previous methods based on FFANet, including contrastive regularization (CR) (Wu et al. 2021), curricular contrastive regularization (CCR) (Zheng et al. 2023), and our self-prior guided negative loss (SPN). The comparative results can be found in Tab. 5. Instead of merely employing low-quality input images as negative samples, CCR achieves significant advancements by utilizing consensus negatives from pre-trained models and the curriculum learning approach. Intriguingly, our SPN outperforms other methods, achieving the best improvement without any additional prior knowledge. In addition, for image super-resolution (Wu, Jiang, and Liu 2023), our model contrastive paradigm again registers the highest gains, as presented in Tab. 5. This consistent performance underscores the fact that our proposed model contrastive paradigm is task-agnostic and highly effective for diverse image restoration tasks.

Ablation Studies

Impact of Negative Model To provide a deeper understanding for the role of our negative model, our ablation study involves the exploration of different configurations of

Method	MIMO-UNet	HINet	MAXIM	Restormer	UFormer	NAFNet	NAFNet+SPN (Ours)
PSNR	32.68	32.71	32.86	32.92	32.97	32.87	32.93(+0.06)
SSIM	0.959	0.959	0.961	0.961	0.967	0.9606	0.9619(+0.0013)

Table 4: **Comparison results of image deblurring.** We take NAFNet (Chen et al. 2022a) as the benchmark and retrain it with the proposed model contrastive paradigm on GoPro dataset.

Methods	Task & Dataset	PSNR	SSIM
FFANet (Qin et al. 2020b)	Image Dehazing (SOTS-indoor)	36.39	0.9886
+CR (Wu et al. 2021)		36.74	0.9906
+CCR (Zheng et al. 2023)		39.24	0.9937
+SPN (Ours)		39.80	0.9947
EDSR (Lim et al. 2017)	SISR (Urban100)	26.04	0.7849
+PCL (Wu, Jiang, and Liu 2023)		26.07	0.7863
+SPN (Ours)		26.12	0.7878

Table 5: A comparative analysis of the existing contrastive paradigms versus our proposed model contrastive approach. Existing methods are task-oriented and proposed for image dehazing and image super-resolution separately. *Our model contrastive paradigm is task-agonist and general to improve diverse image restoration tasks.*

Negative Model	-	Random	Pre-trained	Default
Avg. PSNR	28.46	28.44	28.51	28.55

Table 6: Results of retrained lightweight SwinIR with different negative models.

Step s	100	500	1000	2000	all
FFANet	38.90	38.54	38.27	37.55	39.54

Table 7: Ablation studies of the negative step s . We retrain FFANet with different negative step s on indoor dataset.

the negative model, including an randomly initialized and fixed SwinIR model, a pre-trained and fixed SwinIR model, and our default one. The results of these different configurations, which shed light on the efficacy of our proposed approach, are presented in Tab. 6. '-' presents the baseline model without contrastive negative model. Firstly, negative model with random and fixed parameters can not afford effective negatives and impedes the target SR model. When we set the negative model as the pre-trained and fixed one, it enhances the target model but achieves worse performance than ours. We think the adaptive and curricular negatives generated by model contrastive paradigm is essential to provide a smooth negative regularization, which is consistent with some existing methods.

Impact of Negative Step We conducted an ablation study, where FFANet was retrained with various negative models, each differentiated by its updating iteration, s . The results are tabulated in Tab. 7. It becomes evident that the choice of step s distinctly influences both the negative model and performance. A smaller step provides more challenging negatives compared to the larger step, leading to superior performance. In our experiments, we employ multiple negative models with the four steps together, achieving the best results. The incorporation of multiple negative models ensures a consistent supply of robust negatives.

Impact of Balancing Coefficient We study the influence of the coefficient λ in Eq. (1), and results are presented in Tab. 8, where 0 value means the original L_1 loss with-

λ Value	0	1e-2	1e-3	5e-4	1e-4	1e-5
EDSR-light	28.58	-	-	28.56	28.63	28.60

Table 8: Ablation studies on coefficient in total loss function.

w in EMA	0	0.01	0.1	0.5	0.9	0.999
EDSR-light	-	-	28.63	28.60	26.60	28.61

Table 9: Ablation studies on the updating weight in EMA.

out our negative regularization. When λ set as 1e-2 or 1e-3, there is collapse during training, especially in the early stage. This is reasonable that large negative loss can influence the model updating towards to the optimal direction. When λ is 1e-4, our model contrastive paradigm achieves the best performance. Considering that the proposed model contrastive paradigm is task-agonist and adaptive to various image restoration tasks, in this paper, we take $\lambda = 1e - 4$ as the default value across different tasks.

Impact of Updating Weight in EMA In reference to Eq. (refeq:ema), we examine the influence of varying updating weights. The outcomes are detailed in Tab. 9. In general, a smaller value of w retains less latency information, bringing it in closer alignment with the target model. This results in the generation of the most challenging negatives. The symbol '-' indicates model collapse during training. As w increases, it becomes evident that the optimal performance is attained at $w = 0.1$. Based on our empirical observations, we consistently utilize $w = 0.1$ as the default setting in all subsequent experiments.

Limitation

In this work, we propose a task-agonist, general and adaptive model contrastive paradigm for low-level tasks and further improves existing models. In experiments, we made a considerable effort to validate our approach across diverse tasks and different model architectures. Nevertheless, unexplored areas remain, such as JPEG artifact removal, image denoising, and certain real-world scenarios. In ablation studies, our ablation studies furnished comprehensive insights into the hyper-parameters of our model contrastive paradigm, primarily focusing on image super-resolution tasks, as illustrated in Tables 6 and 7. We do not systematically evaluated these hyper-parameters across each target task to discern potential performance gains. These areas represent promising avenues for future exploration.

Conclusion

In this study, we propose innovative model contrastive paradigm for various low-level tasks. Compared to the task-oriented negatives in existing methods, the proposed model contrastive paradigm, constructing negatives from the target model itself, is task-agonist, general to various image restoration tasks by a Self-Prior guided Negative loss (SPN). Our proposed SPN is straightforward to implement and does

not rely on any task or data prior. We have retrained several image restoration models, and they achieve significant improvements across various tasks and architectures. In the future, we believe it would be meaningful to evaluate our proposed paradigm in more dense prediction tasks, potentially offering fresh insights and advances for the community.

References

- Agustsson, E.; and Timofte, R. 2017. NTIRE 2017 Challenge on Single Image Super-Resolution: Dataset and Study. In *Proceedings of the IEEE Conference on Computer Vision and Pattern Recognition (CVPR) Workshops*.
- Chen, L.; Chu, X.; Zhang, X.; and Sun, J. 2022a. Simple Baselines for Image Restoration. In *Proceedings of the European Conference on Computer Vision (ECCV)*, volume 13667 of *Lecture Notes in Computer Science*, 17–33. Springer.
- Chen, T.; Kornblith, S.; Norouzi, M.; and Hinton, G. E. 2020. A Simple Framework for Contrastive Learning of Visual Representations. In *Proceedings of the International Conference on Machine Learning (ICML)*, volume 119, 1597–1607.
- Chen, X.; and He, K. 2021. Exploring Simple Siamese Representation Learning. In *Proceedings of the IEEE/CVF Conference on Computer Vision and Pattern Recognition (CVPR)*, 15750–15758.
- Chen, X.; Pan, J.; Jiang, K.; Li, Y.; Huang, Y.; Kong, C.; Dai, L.; and Fan, Z. 2022b. Unpaired deep image deraining using dual contrastive learning. In *Proceedings of the IEEE/CVF Conference on Computer Vision and Pattern Recognition (CVPR)*, 2017–2026.
- Dai, T.; Cai, J.; Zhang, Y.; Xia, S.; and Zhang, L. 2019. Second-Order Attention Network for Single Image Super-Resolution. In *Proceedings of the IEEE/CVF Conference on Computer Vision and Pattern Recognition (CVPR)*, 11065–11074.
- Dong, C.; Loy, C. C.; He, K.; and Tang, X. 2016. Image Super-Resolution Using Deep Convolutional Networks. *IEEE Trans. Pattern Anal. Mach. Intell.*, 38: 295–307.
- Dosovitskiy, A.; Beyer, L.; Kolesnikov, A.; Weissenborn, D.; Zhai, X.; Unterthiner, T.; Dehghani, M.; Minderer, M.; Heigold, G.; Gelly, S.; Uszkoreit, J.; and Houtsby, N. 2021. An Image is Worth 16x16 Words: Transformers for Image Recognition at Scale. In *International Conference on Learning Representations (ICLR)*.
- Fu, X.; Huang, J.; Zeng, D.; Huang, Y.; Ding, X.; and Paisley, J. W. 2017. Removing Rain from Single Images via a Deep Detail Network. In *Proceedings of the IEEE/CVF Conference on Computer Vision and Pattern Recognition (CVPR)*, 1715–1723.
- Grill, J.; Strub, F.; Althé, F.; Tallec, C.; and et al. 2020. Bootstrap Your Own Latent - A New Approach to Self-Supervised Learning. In *Advances in Neural Information Processing Systems (NeurIPS)*.
- Gui, J.; Chen, T.; Cao, Q.; Sun, Z.; Luo, H.; and Tao, D. 2023a. A Survey of Self-Supervised Learning from Multiple Perspectives: Algorithms, Theory, Applications and Future Trends. *ArXiv*, abs/2301.05712.
- Gui, J.; Cong, X.; Cao, Y.; Ren, W.; Zhang, J.; Zhang, J.; Cao, J.; and Tao, D. 2023b. A Comprehensive Survey and Taxonomy on Single Image Dehazing Based on Deep Learning. *ACM Comput. Surv.*, 55(13s).
- He, K.; Fan, H.; Wu, Y.; Xie, S.; and Girshick, R. B. 2020. Momentum Contrast for Unsupervised Visual Representation Learning. In *Proceedings of the IEEE Conference on Computer Vision and Pattern Recognition (CVPR)*.
- Hui, Z.; Gao, X.; Yang, Y.; and Wang, X. 2019. Lightweight Image Super-Resolution with Information Multi-distillation Network. In *Proceedings of the 27th ACM International Conference on Multimedia (ACM MM)*, 2024–2032.
- Jiang, J.; Wang, C.; Liu, X.; and Ma, J. 2023. Deep Learning-Based Face Super-Resolution: A Survey. In *ACM Comput. Surv.*, volume 55.
- Jiang, K.; Wang, Z.; Yi, P.; Chen, C.; Huang, B.; Luo, Y.; Ma, J.; and Jiang, J. 2020. Multi-scale progressive fusion network for single image deraining. In *Proceedings of the IEEE/CVF conference on computer vision and pattern recognition (CVPR)*, 8346–8355.
- Jiang, K.; Wang, Z.; Yi, P.; Chen, C.; Wang, Z.; Wang, X.; Jiang, J.; and Lin, C.-W. 2021. Rain-Free and Residue Hand-in-Hand: A Progressive Coupled Network for Real-Time Image Deraining. *IEEE Transactions on Image Processing*, 30: 7404–7418.
- Lamba, M.; and Mitra, K. 2021. Restoring Extremely Dark Images in Real Time. In *Proceedings of the IEEE/CVF Conference on Computer Vision and Pattern Recognition (CVPR)*, 3487–3497. Computer Vision Foundation / IEEE.
- Li, X.; Wu, J.; Lin, Z.; Liu, H.; and Zha, H. 2018a. Recurrent Squeeze-and-Excitation Context Aggregation Net for Single Image Deraining. In *Proceedings of the European Conference on Computer Vision (ECCV)*, volume 11211 of *Lecture Notes in Computer Science*, 262–277. Springer.
- Li, X.; Wu, J.; Lin, Z.; Liu, H.; and Zha, H. 2018b. Recurrent Squeeze-and-Excitation Context Aggregation Net for Single Image Deraining. In *Proceedings of the European Conference on Computer Vision (ECCV)*, volume 11211, 262–277. Springer.
- Liang, J.; Cao, J.; Sun, G.; Zhang, K.; Gool, L. V.; and Timofte, R. 2021. SwinIR: Image Restoration Using Swin Transformer. In *Proceedings of the IEEE/CVF International Conference on Computer Vision (ICCV) Workshops*, 1833–1844.
- Lim, B.; Son, S.; Kim, H.; Nah, S.; and Lee, K. M. 2017. Enhanced Deep Residual Networks for Single Image Super-Resolution. In *Proceedings of the IEEE/CVF Conference on Computer Vision and Pattern Recognition (CVPR) Workshops*, 1132–1140.
- Liu, D.; Wen, B.; Fan, Y.; Loy, C. C.; and Huang, T. S. 2018. Non-Local Recurrent Network for Image Restoration. In *Advances in Neural Information Processing Systems (NeurIPS)*, 1680–1689.
- Liu, X.; Ma, Y.; Shi, Z.; and Chen, J. 2019. GridDehazeNet: Attention-Based Multi-Scale Network for Image Dehazing. *Proceedings of the IEEE/CVF International Conference on Computer Vision (ICCV)*, 7313–7322.
- Liu, Z.; Lin, Y.; Cao, Y.; Hu, H.; Wei, Y.; Zhang, Z.; Lin, S.; and Guo, B. 2021. Swin Transformer: Hierarchical Vision Transformer using Shifted Windows. In *Proceedings of the IEEE International Conference on Computer Vision (ICCV)*, 9992–10002.
- Lu, Y.; Lin, Y.; Wu, H.; Luo, Y.; Zheng, X.; Xiong, H.; and Wang, L. 2023. Priors in Deep Image Restoration and Enhancement: A Survey. *arXiv:2206.02070*.
- Lu, Z.; Li, J.; Liu, H.; Huang, C.; Zhang, L.; and Zeng, T. 2022. Transformer for Single Image Super-Resolution. In *Proceedings of the IEEE/CVF Conference on Computer Vision and Pattern Recognition Workshops (CVPRW)*, 456–465. IEEE.
- Mei, Y.; Fan, Y.; and Zhou, Y. 2021. Image Super-Resolution With Non-Local Sparse Attention. In *Proceedings of the IEEE/CVF Conference on Computer Vision and Pattern Recognition (CVPR)*, 3517–3526.
- Qin, X.; Wang, Z.; Bai, Y.; Xie, X.; and Jia, H. 2020a. FFA-Net: Feature Fusion Attention Network for Single Image Dehazing. In *Proceedings of the AAAI Conference on Artificial Intelligence (AAAI)*, 11908–11915. AAAI Press.

- Qin, X.; Wang, Z.; Bai, Y.; Xie, X.; and Jia, H. 2020b. FFA-Net: Feature fusion attention network for single image dehazing. In *Proceedings of the AAAI conference on artificial intelligence*, volume 34, 11908–11915.
- Ronneberger, O.; Fischer, P.; and Brox, T. 2015. U-net: Convolutional networks for biomedical image segmentation. In *Medical Image Computing and Computer-Assisted Intervention–MICCAI 2015: 18th International Conference, Munich, Germany, October 5–9, 2015, Proceedings, Part III* 18, 234–241. Springer.
- Simonyan, K.; and Zisserman, A. 2015. Very Deep Convolutional Networks for Large-Scale Image Recognition. In *International Conference on Learning Representations (ICLR)*.
- Song, Y.; He, Z.; Qian, H.; and Du, X. 2023. Vision Transformers for Single Image Dehazing. *IEEE Transactions on Image Processing*, 32: 1927–1941.
- Su, J.; Xu, B.; and Yin, H. 2022. A Survey of Deep Learning Approaches to Image Restoration. *Neurocomput.*, 487(C): 46–65.
- Suin, M.; Purohit, K.; and Rajagopalan, A. N. 2020. Spatially-Attentive Patch-Hierarchical Network for Adaptive Motion Deblurring. In *Proceedings of the IEEE/CVF Conference on Computer Vision and Pattern Recognition (CVPR)*, 3603–3612. Computer Vision Foundation / IEEE.
- Wang, H.; Wu, Y.; Li, M.; Zhao, Q.; and Meng, D. 2021a. Survey on rain removal from videos or a single image. In *Science China Information Sciences*, volume 65.
- Wang, L.; Wang, Y.; Dong, X.; Xu, Q.; Yang, J.; An, W.; and Guo, Y. 2021b. Unsupervised degradation representation learning for blind super-resolution. In *Proceedings of the IEEE/CVF Conference on Computer Vision and Pattern Recognition (CVPR)*, 10581–10590.
- Wang, T.; Yang, X.; Xu, K.; Chen, S.; Zhang, Q.; and Lau, R. W. H. 2019a. Spatial Attentive Single-Image Deraining With a High Quality Real Rain Dataset. In *Proceedings of the IEEE/CVF Conference on Computer Vision and Pattern Recognition (CVPR)*, 12270–12279. Computer Vision Foundation / IEEE.
- Wang, T.; Yang, X.; Xu, K.; Chen, S.; Zhang, Q.; and Lau, R. W. H. 2019b. Spatial Attentive Single-Image Deraining With a High Quality Real Rain Dataset. In *Proceedings of the IEEE/CVF Conference on Computer Vision and Pattern Recognition (CVPR)*, 12270–12279. Computer Vision Foundation / IEEE.
- Wang, T.; Zhang, K.; Shen, T.; Luo, W.; Stenger, B.; and Lu, T. 2023. Ultra-High-Definition Low-Light Image Enhancement: A Benchmark and Transformer-Based Method. In *Proceedings of the AAAI Conference on Artificial Intelligence (AAAI)*, 2654–2662. AAAI Press.
- Wang, Z.; Chen, J.; and Hoi, S. C. H. 2021a. Deep Learning for Image Super-Resolution: A Survey. In *IEEE Trans. Pattern Anal. Mach. Intell.*, volume 43, 3365–3387. United States.
- Wang, Z.; Chen, J.; and Hoi, S. C. H. 2021b. Deep Learning for Image Super-Resolution: A Survey. *IEEE Trans. Pattern Anal. Mach. Intell.*, 43(10): 3365–3387.
- Wang, Z.; Cun, X.; Bao, J.; Zhou, W.; Liu, J.; and Li, H. 2022. Uformer: A General U-Shaped Transformer for Image Restoration. In *2022 IEEE/CVF Conference on Computer Vision and Pattern Recognition (CVPR)*, 17662–17672.
- Wu, G.; Jiang, J.; Bai, Y.; and Liu, X. 2023a. Incorporating Transformer Designs into Convolutions for Lightweight Image Super-Resolution. arXiv:2303.14324.
- Wu, G.; Jiang, J.; Jiang, K.; and Liu, X. 2023b. Fully 1×1 Convolutional Network for Lightweight Image Super-Resolution. arXiv:2307.16140.
- Wu, G.; Jiang, J.; and Liu, X. 2023. A Practical Contrastive Learning Framework for Single-Image Super-Resolution. *IEEE Transactions on Neural Networks and Learning Systems*, 1–12.
- Wu, H.; Qu, Y.; Lin, S.; Zhou, J.; Qiao, R.; Zhang, Z.; Xie, Y.; and Ma, L. 2021. Contrastive learning for compact single image dehazing. In *Proceedings of the IEEE/CVF Conference on Computer Vision and Pattern Recognition (CVPR)*, 10551–10560.
- Xiao, J.; Fu, X.; Liu, A.; Wu, F.; and Zha, Z.-J. 2022. Image Deraining Transformer. *IEEE Transactions on Pattern Analysis and Machine Intelligence*, 1–18.
- Yang, W.; Tan, R. T.; Feng, J.; Liu, J.; Guo, Z.; and Yan, S. 2017a. Deep Joint Rain Detection and Removal from a Single Image. In *Proceedings of the IEEE/CVF Conference on Computer Vision and Pattern Recognition (CVPR)*, 1685–1694.
- Yang, W.; Tan, R. T.; Feng, J.; Liu, J.; Guo, Z.; and Yan, S. 2017b. Deep Joint Rain Detection and Removal from a Single Image. In *Proceedings of the IEEE/CVF Conference on Computer Vision and Pattern Recognition (CVPR)*, 1685–1694.
- Yang, W.; Tan, R. T.; Wang, S.; Fang, Y.; and Liu, J. 2021. Single Image Deraining: From Model-Based to Data-Driven and Beyond. *IEEE Transactions on Pattern Analysis and Machine Intelligence*, 43(11): 4059–4077.
- Ye, Y.; Yu, C.; Chang, Y.; Zhu, L.; Zhao, X.-l.; Yan, L.; and Tian, Y. 2022. Unsupervised Deraining: Where Contrastive Learning Meets Self-similarity. In *Proceedings of the IEEE/CVF Conference on Computer Vision and Pattern Recognition (CVPR)*, 5811–5820.
- Zamir, S. W.; Arora, A.; Khan, S.; Hayat, M.; Khan, F. S.; and Yang, M. 2022. Restormer: Efficient Transformer for High-Resolution Image Restoration. In *2022 IEEE/CVF Conference on Computer Vision and Pattern Recognition (CVPR)*, 5718–5729.
- Zhang, K.; Zuo, W.; Chen, Y.; Meng, D.; and Zhang, L. 2017. Beyond a Gaussian Denoiser: Residual Learning of Deep CNN for Image Denoising. *IEEE Trans. Image Process.*, 26(7): 3142–3155.
- Zhang, K.; Zuo, W.; and Zhang, L. 2018. Learning a single convolutional super-resolution network for multiple degradations. In *Proceedings of the IEEE/CVF Conference on Computer Vision and Pattern Recognition (CVPR)*, 3262–3271.
- Zhang, Y.; Li, K.; Li, K.; Wang, L.; Zhong, B.; and Fu, Y. 2018a. Image Super-Resolution Using Very Deep Residual Channel Attention Networks. In *Proceedings of the European conference on computer vision (ECCV)*, 286–301.
- Zhang, Y.; Tian, Y.; Kong, Y.; Zhong, B.; and Fu, Y. 2018b. Residual Dense Network for Image Super-Resolution. In *Proceedings of the IEEE Conference on Computer Vision and Pattern Recognition (CVPR)*, 2472–2481.
- Zheng, Y.; Zhan, J.; He, S.; Dong, J.; and Du, Y. 2023. Curricular contrastive regularization for physics-aware single image dehazing. In *Proceedings of the IEEE/CVF Conference on Computer Vision and Pattern Recognition (CVPR)*, 5785–5794.